High performance $Bi_{0.5}Na_{0.5}TiO_3$-$BiAlO_3$-$K_{0.5}Na_{0.5}NbO_3$ lead-free pyroelectric ceramics for thermal detectors

Zhen Liu, Weijun Ren, Ping Peng, Shaobo Guo, Teng Lu, Yun Liu, Xianlin Dong, and Genshui Wang

Citation: Appl. Phys. Lett. **112**, 142903 (2018); doi: 10.1063/1.5020424
View online: https://doi.org/10.1063/1.5020424
View Table of Contents: http://aip.scitation.org/toc/apl/112/14
Published by the American Institute of Physics

High performance $Bi_{0.5}Na_{0.5}TiO_3$-$BiAlO_3$-$K_{0.5}Na_{0.5}NbO_3$ lead-free pyroelectric ceramics for thermal detectors

Zhen Liu,[1,2,a)] Weijun Ren,[2] Ping Peng,[2] Shaobo Guo,[2] Teng Lu,[1] Yun Liu,[1,a)] Xianlin Dong,[2] and Genshui Wang[2,a)]

[1]*Research School of Chemistry, The Australian National University, Canberra, Australian Capital Territory 2601, Australia*

[2]*Key Laboratory of Inorganic Functional Materials and Devices, Shanghai Institute of Ceramics, Chinese Academy of Sciences, 1295 Dingxi Road, Shanghai 200050, People's Republic of China*

(Received 22 December 2017; accepted 25 March 2018; published online 3 April 2018)

Both high pyroelectric properties and good temperature stability of ferroelectric materials are desirable when used for applications in infrared thermal detectors. In this work, we report lead-free ternary $0.97(0.99Bi_{0.5}Na_{0.5}TiO_3\text{-}0.01BiAlO_3)\text{-}0.03K_{0.5}Na_{0.5}NbO_3$ (BNT-BA-KNN) ceramics, which not only exhibits a large pyroelectric coefficient ($p \sim 3.7 \times 10^{-8}\,C\,cm^{-2}K^{-1}$) and figures of merit ($F_i$, F_v, and F_d) but also shows excellent thermal stable properties. At room temperature, F_i, F_v, and F_d are determined as high as 1.32×10^{-10} m/V, 2.89×10^{-2} m^2/C, and $1.15 \times 10^{-5}\,Pa^{-1/2}$ at 1 kHz and 1.32×10^{-10} m/V, $2.70 \times 10^{-2}\,m^2/C$, and $1.09 \times 10^{-5}\,Pa^{-1/2}$ at 20 Hz, respectively. During the temperature range of RT to 85 °C, the achieved p, F_i, F_v, and F_d do not vary too much. The high depolarization temperature and the undispersed ferroelectric-ergodic relaxor phase transition with a sharp pyroelectric coefficient peak value of $\sim 400 \times 10^{-8}$ $C\,cm^{-2}K^{-1}$ are suggested to be responsible for this thermal stability, which ensures reliable actual operation. The results reveal the BNT-BA-KNN ceramics as promising lead-free candidates for infrared thermal detector applications. *Published by AIP Publishing.* https://doi.org/10.1063/1.5020424

Pyroelectric materials have been of strong interest for the development of thermal based sensors, accelerators, and energy harvesters.[1–5] The utilization of pyroelectric materials for uncooled infrared thermal detectors has recently gained a rapid growth of investigations since they promise a broad wavelength response, high sensitivity, low cost, and elimination of cooling systems. It is general to evaluate pyroelectric ceramics though the figures of merit (FOMs):[5] $F_i = \frac{p}{c_v}$, $F_v = \frac{p}{c_v \varepsilon_0 \varepsilon_r}$, and $F_d = \frac{p}{c_v \sqrt{\varepsilon_0 \varepsilon_r \tan\sigma}}$, where c_v is the volume heat capacity and F_i, F_v, and F_d represent the current responsivity, voltage responsivity, and detectivity, respectively. During the last few decades, lead-based ferroelectric ceramics such as $Pb(Zr,Ti)O_3$ (PZT),[6–8] $Pb(Zr,Sn,Ti)O_3$ (PZST),[9] $Pb(Sc,Ta)O_3$ (PST),[10–12] and $Pb(Mg,Nb)O_3$-$PbTiO_3$ (PMN-PT)[13] were widely investigated for infrared detection due to their superior pyroelectric properties. However, environmental concerns and global restrictions present high demands to eliminate the pollution of lead-containing compounds and develop high-performance lead-free substitutions. By far, many investigations have been carried out on lead-free ferroelectric ceramics for possible pyroelectric based applications. For example, the enhanced pyroelectric coefficient (p) of 1.24×10^{-8} C $cm^{-2}K^{-1}$ and the figure of merit of detectivity (F_d) of $0.61 \times 10^{-5}\,Pa^{-1/2}$ were realized on $Ca_{0.2}Sr_{0.1}Ba_{0.7}Nb_2O_6$ ceramics by Chen *et al.*[14] Moreover, Jiang *et al.*[15] studied the pyroelectric properties of Mn-doped $0.97K_{0.5}Na_{0.5}NbO_3$-$0.03(Bi_{0.5}K_{0.5})TiO_3$ ceramics and achieved p and F_d values of 2.18×10^{-8} C $cm^{-2}K^{-1}$ and $0.571 \times 10^{-5}\,Pa^{-1/2}$, respectively. Srikanth *et al.*[16] also reported $0.6(Ba_{0.9}Ca_{0.1})TiO_3$-$0.4Ba(Sn_{0.2}Ti_{0.8})O_3$ pyroelectric ceramics with an optimized p value of 2.05×10^{-8} C $cm^{-2}K^{-1}$ and an F_d value of $0.41 \times 10^{-5}\,Pa^{-1/2}$. Despite that many progresses have been reported in lead-free pyroelectric materials, they still exhibit far inferiority to these lead-based materials.

Sodium bismuth titanate ($Bi_{0.5}Na_{0.5}TiO_3$, BNT) ceramics exhibit large remanent polarization ($P_r = 38\,\mu C/cm^2$) and high Curie temperature ($T_C = 320$ °C), exhibiting favorable characteristics for pyroelectric applications. However, its large leakage current and high coercive electric field (~7.3 kV/mm) make them difficult to be poled. Forming BNT based solid solutions with other perovskites such as $BaTiO_3$, $BiAlO_3$, and $(Bi,K)TiO_3$ not only improves the poling effectiveness but also offers great opportunities for tuning their ferroelectric properties.[17–20] To fit for real pyroelectric applications, the BNT family must satisfy two aspects of requirements. One is high pyroelectric performance at room temperature, including pyroelectric coefficients and various figures of merit. On the other hand, the good temperature stability of p and FOMs is also inevitable to ensure their reliable operation. Recently, Sun *et al.*[21] reported that Mn doped $0.946Bi_{0.5}Na_{0.5}TiO_3$-$0.054BaTiO_3$ (BNT-BT) single crystals with the (111) orientation possess high pyroelectric coefficients and large figures of merit. The value of p can reach as high as 5.88×10^{-8} C $cm^{-2}K^{-1}$ and does not increase too much with temperature varying from 20 °C to 85 °C. However, for their ceramics counterparts, although a large p value of 5.7×10^{-8} C $cm^{-2}K^{-1}$ was realized by Guo *et al.*[22] on $0.93Bi_{0.5}Na_{0.5}TiO_3$-$0.07Ba(Zr_{0.055}Ti_{0.945})O_3$ (BNT-BZT) pyroelectric ceramics near the morphotropic phase boundary (MPB), the value of p

a)Authors to whom correspondence should be addressed: zhenliumse@163.com; yun.liu@anu.edu.au; and genshuiwang@mail.sic.ac.cn.

soared to 20.6×10^{-8} C cm^{-2}K^{-1} with temperature increasing to 50 °C. Quite recently, Balakt *et al.*[23] obtained even higher p of 7.42×10^{-8} C cm^{-2}K^{-1} at room temperature on La doped $0.94Bi_{0.5}Na_{0.5}TiO_3$-$0.06BaTiO_3$ ceramics. However, the great enhancement of p was realized at the expense of bringing the depolarization temperature (T_d) down to near room temperature, which will also result in the temperature instability. Moreover, the ceramics will experience polarization loss during the heat-involved manufacture procedures, thus affecting their reusability, which limits their applicability as well. Therefore, BNT based ceramics possessing both high pyroelectric properties and favorable thermal stability necessarily deserve further research.

In present work, a potential lead-free pyroelectric ceramics was presented for thermal detectors. A large pyroelectric coefficient of 3.9×10^{-8} C cm^{-2}K^{-1} and enhanced FOMs were achieved at room temperature in $0.97(0.99Bi_{0.5}Na_{0.5}TiO_3$-$0.01BiAlO_3)$-$0.03K_{0.5}Na_{0.5}NbO_3$ (BNT-BA-KNN) ceramics. Moreover, the obtained p and FOMs demonstrate good temperature stability over a wide temperature range of RT to 85 °C. The high depolarization temperature and undispersed ferroelectric-relaxor phase transition of BNT-BA-KNN are suggested to be responsible for the improvement. Our results reveal the great potential of BNT-BA-KNN ceramics for infrared thermal detector applications.

The BNT-BA-KNN ceramics were prepared through a conventional solid-state reaction method. $BiAlO_3$ (BA) was chosen due to its ability to improve the polarization of BNT.[18] $K_{0.5}Na_{0.5}NbO_3$ (KNN) was added since it was widely used to tune the depolarization temperature of BNT-based materials.[24] Bi_2O_3 (99.9%), TiO_2 (99.8%), Na_2CO_3 (99.8%), Al_2O_3 (99%), K_2CO_3 (99%), and Nb_2O_5 (99.9%) were used as the starting raw materials. The mixed oxides were calcined at 850 °C for 2 h and sintered at 1180 °C for 2 h in a covered alumina crucible. To minimize the evaporation of the volatile elements Bi, Na, and K, the disks were embedded in atmospheric powder of the same composition. The samples were ground to disks with a thickness of 0.5 mm and a diameter of 8 mm. Both sides of the disks were coated with a thin layer of silver paste with a diameter of 7.8 mm through screen printing and were fired at 700 °C for 30 min.

The crystal structure of the as-sintered ceramics was characterized using an X-ray diffractometer (XRD, D8 Advance, Bruker, Karlsruhe, Germany), operated with Cu Ka radiation at room temperature (~30 °C). The microstructure of the ceramics was taken using a field emission scanning electron microscope (FE-SEM, S-4800, Hitachi, Japan). For dielectric and pyroelectric measurements, the samples were poled in silicone oil under an electric field of 7 kV/mm at 100 °C for 30 min and then cooled to room temperature without electric field removal to make sure that the samples were fully poled. The dielectric constant (ε_r) and dielectric loss ($\tan\delta$) were measured using a Hewlett Packard LCR meter with a heating rate of 2 °C/min at 100 Hz, 1 kHz, 10 kHz, 100 kHz, and 1 MHz. The frequency dependent ε_r and $tan\delta$ were measured at room temperature from 20 Hz to 10 kHz. The polarization-electric field (P-E) loops were characterized at 1 Hz using an aix ACCT TF 2000 analyzer ferroelectric measuring system (aix ACCT Co., Aachen, Germany). The pyroelectric coefficient was measured by the Byer-Roundy method as a function of temperature.[25] The pyroelectric current was recorded with a Keithley 6517A electrometer/high resistance meter for poled samples both on heating and cooling with a rate of 2 °C/min.

Figure 1 shows the XRD pattern of BNT-BA-KNN ceramics, and the inset illustrates the surface microstructure of the as-sintered samples. The XRD result confirms that the ceramics are crystallized into a perovskite structure. A small trace of the bismuth-deficient $Bi_2Al_4O_9$ secondary phase was detected at around $2\theta = 29°$, which was also observed previously in BNT-BA ceramics.[18] The amount of the impurity phase is calculated to be around 0.32 mol. % through integrating the related peaks. The samples exhibit a dense and void-free microstructure, and the grain sizes vary from 1 to 6 μm. This is consistent with the high relative density (>97%) determined by the Archimedes method.

Figure 2(a) presents the temperature dependent dielectric constant (ε_r) and dielectric loss ($\tan\delta$) of pre-poled BNT-BA-KNN ceramics measured at different frequencies from room temperature to 400 °C. A general frequency-dispersion is clearly visible for both ε_r and $\tan\delta$, which indicates their relaxor characteristic.[26] As temperature increases, three anomalies can be detected, similar to previous reports.[27] The first characteristic temperature $T_{F\text{-}R}$ can be determined by the frequency-independent dielectric loss peak and dielectric constant inflection point at 118 °C, which denotes the transition from ferroelectric to the ergodic relaxor (FE-ER) phase with increasing temperature, as supported by the temperature dependent polarization hysteresis measurements in Fig. 2(b) and the TEM study.[28,29] The FE-ER phase transition will result in reoriented dipoles and a significant reduction in remanent polarization. Thus, $T_{F\text{-}R}$ had also been regarded as the depolarization temperature T_d.[30,31] The second transition temperature is characterized by the frequency dispersion vanishing point at 225 °C. The third transition temperature T_m happens at the maximum dielectric constant, which provides the evolution to the paraelectric phase. Although many works have been performed with regard to the temperature dependent evolutions of the BNT family, the structural variations during these phase transitions still remain controversy.

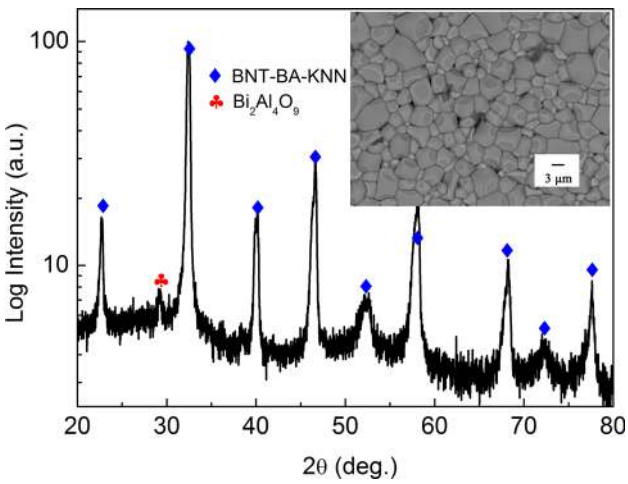

FIG. 1. The XRD pattern of as-sintered BNT-BA-KNN ceramics. The inset illustrates the surface microstructure of the sample.

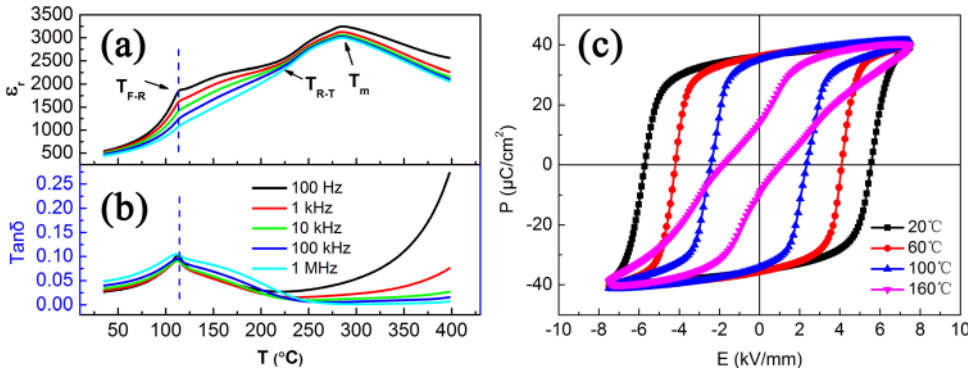

FIG. 2. (a) Temperature dependent dielectric constant and dielectric loss of poled BNT-BA-KNN ceramics at 100 Hz, 1 kHz, 10 kHz, 100 kHz, and 1 MHz. (b) *P-E* loops of BNT-BA-KNN ceramics at different temperatures at 1 Hz.

For pyroelectric applications, it is important to evaluate the dielectric properties at lower frequencies of <100 Hz. However, previous studies performed on the BNT-based ceramics usually report the dielectric properties at higher frequencies. Figure 3 shows the f dependent dielectric constant and loss of poled BNT-BA-KNN ceramics at room temperature during the f range of 20–10 kHz. It can be seen that as f decreases from 10 kHz to 20 Hz, ε_r slightly increases and $\tan\delta$ decreases slightly first and then increases slightly. To be specific, ε_r is 514, 536, and 551 and $\tan\delta$ is 0.029, 0.028, and 0.030 at 1 kHz, 100 Hz, 20 Hz, respectively. The relatively stable dielectric parameters at lower frequencies are favorable for their potential pyroelectric applications.

Figure 4 shows the temperature dependent pyroelectric coefficient on heating calculated according to the following definition:[22]

$$p = \frac{dP_r}{dT} = \frac{I(T)}{A \cdot (dT/dt)}, \tag{1}$$

where $I(T)$ represents the pyroelectric current, A is the electrode area of the sample, and dT/dt is the heating rate. At room temperature, a large p value of 3.9×10^{-8} C cm^{-2}K^{-1} upon heating is achieved, which is comparable to the commercially used PZT pyroelectric ceramics.[5] The room temperature p upon cooling is also measured to be as large as 3.5×10^{-8} C cm^{-2}K^{-1}. It should also be noted that due to the higher T_d, the p value obtained here is slightly lower than that of BNT-BZT[22] and La-doped BNT-BT.[23] However, a high T_d is necessary because it defines the upper limit temperature of real pyroelectric-based applications. From the peak of the pyroelectric curve, T_d is determined as 118 °C, which equals the value of T_{F-R} recorded from the ε_r-T and $\tan\delta$-T curves. This is different from the situation of BNT-BT, for which T_d measured from the pyroelectric current curve locates 10 °C lower than T_{F-R} recorded from dielectric measurements.[32] At T_d, the peak value of the pyroelectric coefficient reaches as high as 400×10^{-8} C cm^{-2}K^{-1}. Although this large p itself is unusable for practical pyroelectric applications due to the irreversibility of the depolarization transition during cooling, the sharp pyroelectric coefficient indicates the undispersed ferroelectric-ergodic relaxor phase transition process, which is helpful for stabilizing the pyroelectric properties when T is lower than T_d.

The inset of Fig. 4 presents the calculated remanent polarization (P_r) of poled BNT-BA-KNN ceramics as a function of temperature. P_r is achieved by integration of depolarization current according to the following equation:

$$P_r = \int_{T_1}^{T_2} p dT = \int_{T_1}^{T_2} \frac{I(T)}{A \cdot (dT/dt)} dT, \tag{2}$$

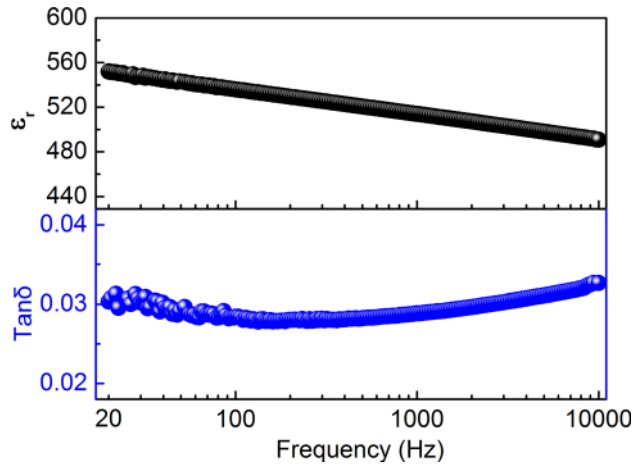

FIG. 3. The frequency dependent dielectric constant and loss at room temperature during the range of 20 Hz–10 kHz.

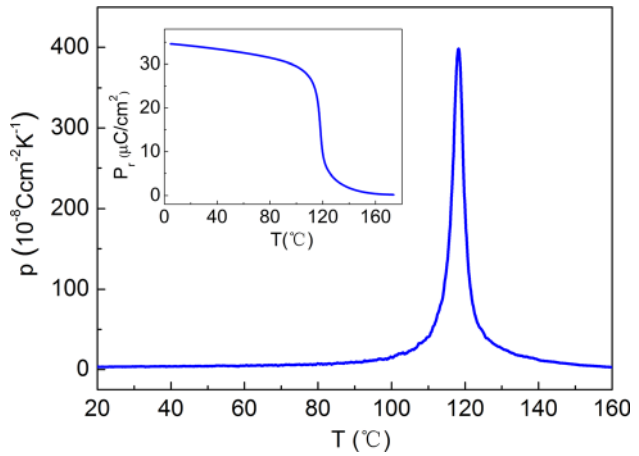

FIG. 4. The pyroelectric coefficient of the poled BNT-BA-KNN ceramics with the increasing temperature rate of 2 °C/min. The inset shows the remanent polarization as a function of temperature.

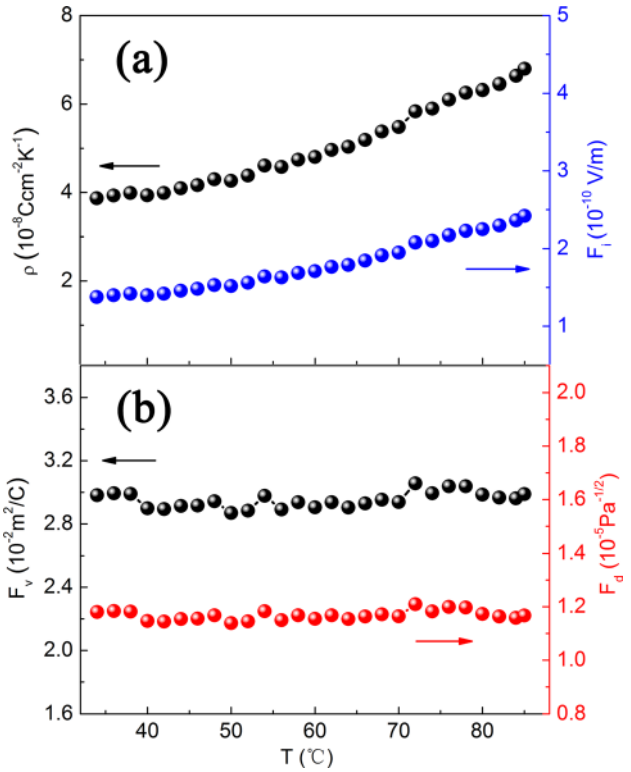

FIG. 5. Pyroelectric coefficient p and figures of merit F_i, F_v, and F_d as a function of temperature on heating at 1 kHz during the range of RT to 85 °C.

where T_1 and T_2 represent the lower and the upper temperature, respectively. At room temperature, P_r is determined to be 34.6 μC/cm^2, which is consistent with the values recorded from P-E loops in Fig. 2(b). Also, it can be seen that P_r slightly decreases from 34.6 μC/cm^2 to 29.5 μC/cm^2, when temperature increases from 5 °C to 100 °C. Note that the variation of P_r is less than 15% during this temperature scope. This shows that the ceramics can maintain a stable poled state in a wide temperature window. This is desirable for pyroelectric materials to be used as infrared thermal detectors. When T further increases to near 120 °C, a sudden decline of P_r occurs due to the temperature induced ferroelectric-relaxor phase transition, accompanied by the above-discussed sharp pyroelectric peak.

Figure 5 displays the temperature dependent p and FOMs of BNT-BA-KNN ceramics on heating at 1 kHz in the range of RT to 85 °C. The p and calculated FOMs of BNT-BA-KNN ceramics at 1 kHz, 100 Hz, and 20 Hz are also given in Table I. Note that an average p value of 3.7×10^{-8} C cm^{-2}K^{-1} on heating and cooling is used in this table to calculate the FOMs at different frequencies. Besides BNT-BA-KNN, pyroelectric parameters of other lead-free materials and lead-containing pyroelectric ceramics are also summarized in Table I for comparison. It is obviously seen that the overall pyroelectric properties of BNT-BA-KNN ceramics are much better than those of other lead-free

TABLE I. A comparison of pyroelectric parameters of the BNT-BA-KNN ceramics, other lead-free materials, and lead-containing ceramics.

Material	ε_r	tan δ	*Freq.* (Hz)	T_d (°C)	T_m (°C)	p (10^{-8} C cm^{-2} K^{-1})	F_i (10^{-10} m/V)	F_v (10^{-2} m^2/C)	F_d (10^{-5} Pa$^{-1/2}$)	Reference
BNT-BA-KNN[a]	514	0.029	1k	118	282	3.7	1.32	2.89	1.15	This work
BNT-BA-KNN[a]	536	0.028	100	118	282	3.7	1.32	2.78	1.14	This work
BNT-BA-KNN[a]	551	0.030	20	118	…	3.7	1.32	2.70	1.09	This work
CSBN[b]	328.7	0.033	1k	200	218	1.24	0.60	2.03	0.61	14
SBN[c]	1024	0.033	100	…	90	2.05	0.98	1.08	0.56	33
SBN[d]	1700	…	…	…	60	11	…	…	…	34
KNN-based[e]	980	0.035	100	…	360	2.18	0.994	1.14	0.571	15
KNN-based[f]	1520	0.018	100	…	…	1.90	0.931	0.7	0.598	35
BCT-BST[g]	3500	0.025	1k	…	75	2.05	1.00	0.32	0.41	16
BNT-BZT[h]	1052	0.040	1k	87	…	5.7	2.03	2.18	1.05	22
BNT-BT-ST[i]	1278	0.109	1M	…	184	5.7	2.08	1.8	0.589	36
BNT-BT[j]	671	0.042	1k	54.9	…	12.92	4.61	0.078	2.76	37
BNT-BT[k]	835	0.010	100	120	280	3.80	1.315	2.0	1.56	21
TGS[l]	55	0.025	1k	…	49	5.5	2.12	43	6.1	5
$LiTaO_3$[m]	47	0.005	…	…	665	2.3	0.72	17	35.2–4.9	5
PZT-PMN[n]	196	0.014	33	118	258	3.16	…	7.3	4.33	8
PZ-based[o]	290	0.0027	1590	…	230	3.7	…	6	5.8	7

[a] $0.97(0.99Bi_{0.5}Na_{0.5}TiO_3\text{-}0.01BiAlO_3)\text{-}0.03K_{0.5}Na_{0.5}NbO_3$ ceramics.
[b] $Ca_{0.2}Sr_{0.1}Ba_{0.7}Nb_2O_6$ ceramics.
[c] $Sr_{0.5}Ba_{0.5}Nb_2O_6$ ceramics.
[d] $Sr_{0.67}Ba_{0.33}Nb_2O_6$ crystals.
[e] Mn-doped $0.97K_{0.5}Na_{0.5}NbO_3\text{-}0.03(Bi_{0.5}K_{0.5})TiO_3$ ceramics.
[f] $[(K_{0.5}Na_{0.5})_{0.96}Li_{0.04}](Nb_{0.84}Ta_{0.1}Sb_{0.06})O_3$ ceramics.
[g] $0.6(Ba_{0.9}Ca_{0.1})TiO_3\text{-}0.4Ba(Sn_{0.2}Ti_{0.8})O_3$ ceramics.
[h] $0.93(Bi_{0.5}Na_{0.5})TiO_3\text{-}0.07Ba(Zr_{0.055}Ti_{0.945})O_3$ ceramics.
[i] $0.71(Bi_{0.5}Na_{0.5})TiO_3\text{-}0.065BaTiO_3\text{-}0.22SrTiO_3$ ceramics.
[j] La,Ta-$0.94(Bi_{0.5}Na_{0.5})TiO_3\text{-}0.06BaTiO_3$ ceramics.
[k] Mn-doped $0.946Na_{0.5}Bi_{0.5}TiO_3\text{-}0.054BaTiO_3$ crystals.
[l] TGS crystals.
[m] $LiTaO_3$ crystals.
[n] Mn-doped $0.975Pb(Zr_{0.875}Ti_{0.125})O_3\text{-}0.025Pb(Mg_{1/3}Nb_{2/3})O_3$ ceramics.
[o] Fe, Nb, Ti, U-doped $PbZrO_3$ ceramics.

pyroelectric ceramics. At room temperature, the obtained F_i, F_v, and F_d of BNT-BA-KNN can be as high as 1.32×10^{-10} m/V, 2.89×10^{-2} m^2/C, and 1.15×10^{-5} Pa$^{-1/2}$ at 1 kHz and 1.32×10^{-10} m/V, 2.70×10^{-2} m^2/C, and 1.09×10^{-5} Pa$^{-1/2}$ at 20 Hz, respectively. The high pyroelectric coefficient and the relatively lower dielectric constant (~500) and lower dielectric loss (~0.03) compared with other lead-free ceramics all contribute to the enhancement of FOMs. More importantly, the value of p, F_i, F_v, and F_d can remain relatively stable in the studied temperature scope of RT to 85 °C. Specifically, F_v and F_d vary only ±2%. It should be stressed that although the room temperature p is a bit smaller than those obtained in 0.93BNT-0.07BZT[22] and La-doped BNT-BT,[23] the good temperature stability during the wide temperature range together with the higher FOMs of BNT-BA-KNN pyroelectric ceramics is powerfully in favor of their applicability.

In summary, the microstructure, dielectric, and pyroelectric properties of ternary lead-free $0.97(0.99Bi_{0.5}Na_{0.5}TiO_3$-$0.01BiAlO_3)$-$0.03K_{0.5}Na_{0.5}NbO_3$ ceramics were studied in this work. The dielectric and pyroelectric measurements for poled BNT-BA-KNN ceramics confirm the depolarization temperature as 118 °C. The room temperature p, F_i, F_v, and F_d can reach 3.7×10^{-8} C cm^{-2} K^{-1}, 1.32×10^{-10} m/V, 2.89×10^{-2} m^2/C, and 1.15×10^{-5} Pa$^{-1/2}$ at 1 kHz, respectively. At depolarization temperature, a large and sharp pyroelectric coefficient of 400×10^{-8} C cm^{-2} K^{-1} was also obtained due to the ferroelectric-ergodic relaxor phase transition. The sharp p peak and high T_d contribute to the temperature stability of pyroelectric properties. The values of the voltage responsivity and detectivity can maintain good stability with a variation of ±2%. The overall excellent pyroelectric performance of the BNT-BA-KNN indicates that the ceramics should be promising lead-free alternatives which have great potential for uncooled infrared detector applications.

This work was supported by the Chinese Academy of Sciences Research Equipment Development Project (No. YZ201332), the National Natural Science Foundation (NSFC) of China (No. 61475176), the Shanghai International Science and Technology Cooperation Project (Grant No. 13520700700), and the International Partnership Project of Chinese Academy of Science. Zhen Liu also acknowledges the support of the Shanghai Sailing Program (No. 17YF1429700).

[1]C. R. Bowen, J. Taylor, E. Leboulbar, D. Zabek, A. Chauhan, and R. Vaish, Energy Environ. Sci. **7**, 3836 (2014).
[2]A. V. Shchagin, V. S. Miroshnik, V. I. Volkov, and A. N. Oleinik, Appl. Phys. Lett. **107**, 233505 (2015).
[3]G. Vats, A. Kumar, N. Ortega, C. R. Bowen, and R. S. Katiyar, Energy Environ. Sci. **9**, 1335 (2016).
[4]R. B. Olsen, D. A. Bruno, and J. M. Briscoe, J. Appl. Phys. **58**, 4709 (1985).
[5]R. W. Whatmore, Rep. Prog. Phys. **49**, 1335 (1986).
[6]A. Peláiz-Barranco, A. C. Garcia-Wong, Y. González-Abreu, and J. D. S. Guerra, J. Appl. Phys. **113**, 044104 (2013).
[7]R. W. Whatmore and F. W. Ainger, Proc. SPIE **395**, 261 (1983).
[8]C. P. Shaw, S. Gupta, S. B. Stringfellow, A. Navarro, J. R. Alcock, and R. W. Whatmore, J. Eur. Ceram. Soc. **22**, 2123 (2002).
[9]Q. Zhang, S. Chen, M. Fan, S. Jiang, T. Yang, J. Wang, G. Li, and X. Yao, Mater. Res. Bull. **47**, 4503 (2012).
[10]W. Liu, G. Wang, S. Cao, C. Mao, C. Yao, F. Cao, and X. Dong, J. Am. Ceram. Soc. **93**, 4030 (2010).
[11]C. Zhili, X. Yao, and L. E. Cross, Ferroelectrics **44**, 271 (1983).
[12]N. M. Shorrocks, R. W. Whatmore, and P. C. Osbond, Ferroelectrics **106**, 387 (1990).
[13]S. W. Choi, R. T. R. Shrout, S. J. Jang, and A. S. Bhalla, Ferroelectrics **100**, 29 (1989).
[14]H. Chen, S. Guo, X. Dong, F. Cao, C. Mao, and G. Wang, J. Alloys Compd. **695**, 2723 (2017).
[15]X. P. Jiang, Y. Chen, K. H. Lam, S. H. Choy, and J. Wang, J. Alloys Compd. **506**, 323 (2010).
[16]K. S. Srikanth, S. Patel, S. Steiner, and R. Vaish, Scr. Mater. **146**, 146 (2018).
[17]Y. Guo, Y. Liu, R. L. Withers, F. Brink, and H. Chen, Chem. Mater. **23**, 219 (2011).
[18]H. Yu and Z.-G. Ye, Appl. Phys. Lett. **93**, 112902 (2008).
[19]Z. Liu, W. Ren, H. Nie, P. Peng, Y. Liu, X. Dong, F. Cao, and G. Wang, Appl. Phys. Lett. **110**, 212901 (2017).
[20]Y. Guo, M. Gu, H. Luo, Y. Liu, and R. L. Withers, Phys. Rev. B **83**, 054118 (2011).
[21]R. Sun, J. Wang, F. Wang, T. Feng, Y. Li, Z. Chi, X. Zhao, and H. Luo, J. Appl. Phys. **115**, 074101 (2014).
[22]F. Guo, B. Yang, S. Zhang, F. Wu, D. Liu, P. Hu, Y. Sun, D. Wang, and W. Cao, Appl. Phys. Lett. **103**, 182906 (2013).
[23]A. M. Balakt, C. P. Shaw, and Q. Zhang, J. Eur. Ceram. Soc. **37**, 1459 (2017).
[24]A. Singh and R. Chatterjee, J. Appl. Phys. **109**, 024105 (2011).
[25]R. L. Byer and C. B. Roundy, Ferroelectrics **3**, 333 (1972).
[26]J. E. Daniels, W. Jo, J. Rödel, D. Rytz, and W. Donner, Appl. Phys. Lett. **98**, 252904 (2011).
[27]P. Peng, H. Nie, Z. Liu, W. Ren, F. Cao, G. Wang, and X. Dong, J. Am. Ceram. Soc. **100**, 1030 (2017).
[28]W. Jo, S. Schaab, E. Sapper, L. A. Schmitt, H. Kleebe, A. J. Bell, and J. Rödel, J. Appl. Phys. **110**, 074106 (2011).
[29]C. Ma, X. Tan, and H. J. Kleebe, J. Am. Ceram. Soc. **94**, 4040 (2011).
[30]F. Wang, M. Xu, Y. Tan, T. Wang, W. Shi, and C. Leung, J. Am. Ceram. Soc. **95**, 1955 (2012).
[31]W. Peng, C. Mao, Z. Liu, X. Dong, F. Cao, and G. Wang, Appl. Phys. Lett. **106**, 092903 (2015).
[32]W. Jo, J. Daniels, D. Damjanovic, W. Kleemann, and J. Rödel, Appl. Phys. Lett. **102**, 192903 (2013).
[33]J. Zhang, X. Dong, F. Cao, S. Guo, and G. Wang, Appl. Phys. Lett. **102**, 102908 (2013).
[34]A. M. Glass, Appl. Phys. Lett. **13**, 147 (1968).
[35]S. T. Lau, C. H. Cheng, S. H. Choy, D. M. Lin, K. W. Kwok, and H. L. W. Chan, J. Appl. Phys. **103**, 104105 (2008).
[36]S. Patel, A. Chauhan, S. Kundu, N. A. Madhar, B. Ilahi, R. Vaish, and K. B. R. Varma, AIP Adv. **5**, 087145 (2015).
[37]A. M. Balakt, C. P. Shaw, and Q. Zhang, J. Alloys Compd. **709**, 82 (2017).